Nanoalloy Formation of Ta-containing Trimetallic Small Clusters

ARTICLE *in* THE JOURNAL OF PHYSICAL CHEMISTRY A · FEBRUARY 2011

Impact Factor: 2.69 · DOI: 10.1021/jp1095932 · Source: PubMed

5 AUTHORS, INCLUDING:

Ken Miyajima
The University of Tokyo
54 PUBLICATIONS **1,152** CITATIONS

SEE PROFILE

THE JOURNAL OF PHYSICAL CHEMISTRY A

ARTICLE

pubs.acs.org/JPCA

Nanoalloy Formation of Ta-containing Trimetallic Small Clusters

Ken Miyajima, Hidenori Himeno, Akira Yamada, Hirotaka Yamamoto, and Fumitaka Mafuné*

Department of Basic Science, Graduate School of Arts and Sciences, The University of Tokyo, Komaba, Meguro-ku, Tokyo 153-8902, Japan

ABSTRACT: Trimetallic cluster ions containing Ta and other metal elements were prepared in the gas phase by a triple laser-ablation technique in a controlled manner. We have measured the abundances and their thermal stabilities, using time-of-flight mass spectrometry. Taking advantage of specific abundance distribution of the trimetallic cluster ions (magic stoichiometry), relative to the distinguished stabilities, the coalescence or the segregation of Ta and the other elements in the subnanometer sized clusters was discussed. We found that Nb, W, and Mo, which are categorized as elements with a high heat of vaporization, readily coalesce with Ta, while V, Al, Co, and Pt, which are categorized as elements with a low heat of vaporization, tend to be segregated from Ta. Our experiments, along with the calculation by another research group, suggest that the binding energies of atoms are related to the coalescence or segregation of clusters in the gas phase.

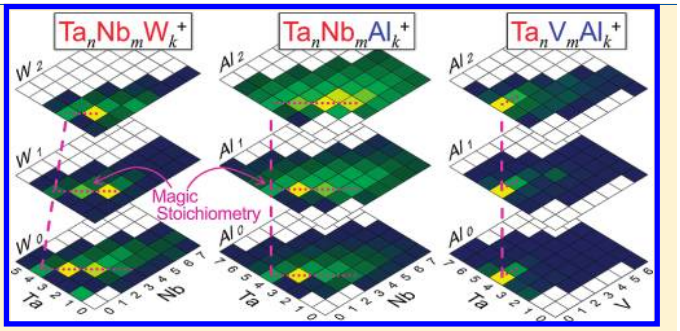

INTRODUCTION

The Hume−Rothery rules are a set of rules that describe the conditions under which an element can dissolve in a bulk metal.[1−3] The rules suggest that the alloy is formed if the atomic sizes, electronegativities, and valencies of the elements are similar and the crystal structure of the bulk metal is shared by the two elements. Although the rules have been widely used for the bulk materials since the 1930s, there is no established conception about whether the rules are valid for subnanometer-sized particles that are composed of several atoms.

In our previous study, we examined whether the rules hold for metal clusters.[4] It is known that Ta_4^+ is one of the most-stable cluster ions in Ta_n^+.[5] We prepared bimetallic cluster ions of Ta and other transition-metal elements (M) in the gas phase using a double laser-ablation technique, and we measured the abundance of $Ta_nM_m^+$ ($n, m = 0, 1, 2, 3, ...$). It was found that Nb, Mo, and W (group A elements) readily form stable $Ta_nM_m^+$ ($n + m = 4$), whereas Ag, Al, Au, Co, Cu, Fe, Hf, Ni, Pt, Ti, and V (group B elements) tend to form $Ta_4M_m^+$ ($m = 0, 1, 2, 3, ...$). The formation of stable $Ta_nM_m^+$ ($n + m = 4$) suggests that a group A atom can replace the Ta atom in Ta_4^+, maintaining its stability. Hence, we can suggest that the group A elements coalesce with Ta. In contrast, the formation of stable $Ta_4M_m^+$ suggests that a group B atom tends to reside outside of the stable Ta_4^+ structure. Hence, we can suggest that the group B elements segregate with Ta. Because the group A elements exhibit a high molar heat of vaporization, it was concluded that the molar heat of vaporization is considered to be a better parameter than electronegativity to categorize the elements for coalescence or segregation in the subnanometer region.

In the present study, we examined whether the rules proposed in the previous study hold for trimetallic clusters. Our interest is especially directed toward the stability of trimetallic clusters that consist of group A atoms or both group A and group B atoms. We discuss the relationship between the stability and structures of the clusters based on the density functional theory (DFT) calculations and thermal fragmentation experiments.

EXPERIMENTAL SECTION

Figure 1 shows an experimental setup used in the present study. Trimetallic clusters were formed in a triple laser ablation source coupled with a reflectron-equipped time-of-flight (TOF) mass spectrometer. A tantalum rod and other metal rods were set downstream of the supersonic source from a solenoid pulsed valve (General Valve). All three rods (5 mm in diameter) were kept rotating and sliding inside a stainless steel block, to maintain the stable laser ablation condition.[6] The rods were irradiated with focused laser pulses (~10 mJ/pulse) at 532 nm from Quanta Ray GCR-130, Continuum Surelite II and Quanta Ray GCR-11 Nd:YAG lasers, which were used to generate the plasma. The evaporated Ta and other metal atoms were cooled in a cylindrical channel (6 mm in diameter and 16 mm long) by the helium gas (>99.99995%) from the valve, forming neutral and charged clusters. We confirmed that essentially the same clusters were formed with the identical size distribution when the positions of the three rods were exchanged. The clusters then were passed through a condensation tube 2 mm in diameter and 60 mm long and an extension tube 4 mm in diameter and 120 mm long with a resistive heater before expansion into the first vacuum chamber, and they were introduced into the differentially pumped second

Received: October 6, 2010
Revised: January 17, 2011
Published: February 15, 2011

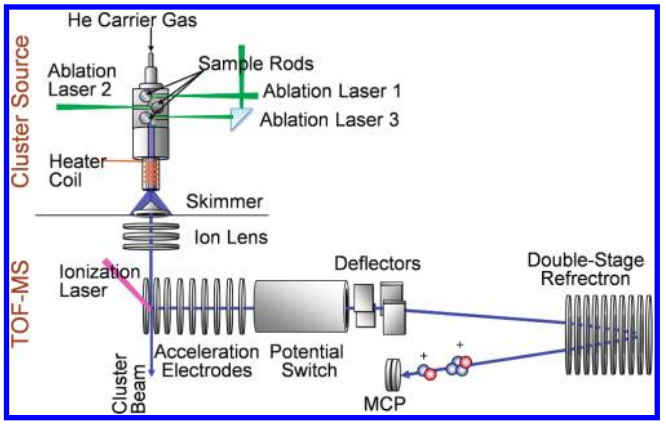

Figure 1. Experimental setup used in the present study.

chamber through a skimmer. Timings of the laser pulses and the valve needed to be carefully controlled, so that clusters could form abundantly and the pulse−pulse fluctuations could be avoided. Hence, we used three separate pulsed lasers for the laser ablation of three metal rods.

The native ions were accelerated orthogonally by the pulsed electric field for the TOF mass analysis after they entered between a repeller and a first electrode. The ions gained the kinetic energy of ~3.4 keV in the acceleration region and were steered and focused by a set of vertical and horizontal deflectors and an einzel lens. After traveling in a 1-m field-free region, the ions were reversed by the reflectron and were detected by a Hamamatsu double-microchannel plate detector. Signals from the detector were amplified by a Stanford SR445A 350 MHz preamplifier and were digitized using an oscilloscope (LeCroy LT344L). Averaged TOF spectra (typically 1000 sweeps) are sent to a personal computer (PC) for analysis via general purpose interface bus (GPIB). The mass resolution, $m/\Delta m$, exceeds 1000.

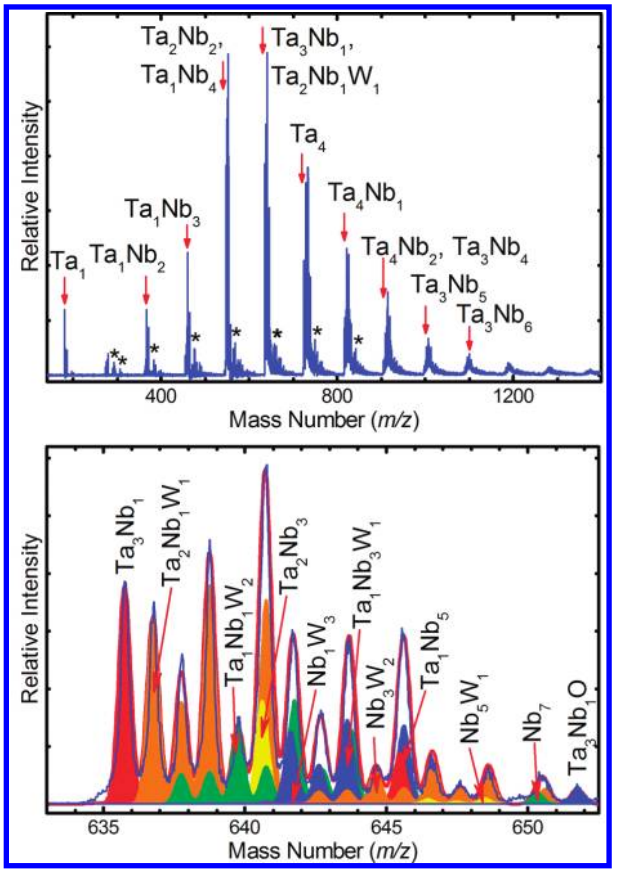

Figure 2. (a) Mass spectrum of $Ta_nNb_mW_k^+$. The ion peaks marked by asterisks are assigned to oxides. (b) Peaks in the mass region from 633 to 652 are assigned as indicated. Observed and simulated spectra are exhibited by a blue line and a red thick line, respectively. The simulated spectrum was obtained by summing the mass peak intensities of clusters. Contribution of each cluster to the mass peaks is shown by the filled peaks with various colors.

RESULTS AND DISCUSSION

Abundance of Nascent Cluster Cations. Figure 2 shows the mass spectrum of $Ta_nNb_mW_k^+$ formed in the gas phase. Because tungsten has several isotopes and the atomic weights of Ta and W are very close, many mass peaks are bunched and overlapped (see Figure 2b). We assigned peaks and determined the abundances of clusters, taking the natural abundance of isotopes into consideration. Care has been taken to discriminate the corresponding oxide clusters.

We exhibited the abundance of the trimetallic cluster ions as color codes in a map. Figure 3a shows the abundance of $Ta_nNb_mW_k^+$. Here, both the Nb and W atoms belong to the group A elements. The cross-sectional plot at $k = 0$, which shows the abundance of $Ta_nNb_m^+$ for n and m, suggests that there is a diagonal line at $n + m = 4$. The line indicates that $Ta_nNb_m^+$ compounds with $n + m = 4$ ($n = 1$, 2, 3, and 4) were abundantly produced in the gas phase (magic stoichiometry). Similarly, in the cross-sectional plot at $k = 1$, which shows the abundance of $Ta_nNb_mW^+$ for n and m, there appears a diagonal line at $n + m = 3$. The line indicates that $Ta_nNb_mW^+$ for $n + m = 3$ is the magic stoichiometry. It is also likely that $n + m = 2$ is the magic stoichiometry for $k = 2$. These findings suggest that, in summary, $n + m + k = 4$ is the magic stoichiometry for $Ta_nNb_mW_k^+$. As mentioned in the former section, Ta_4^+ is one of the most-stable clusters in the small Ta cluster ions. $Ta_nNb_mW_k^+$ ($n + m + k = 4$, with $n \geq 1$), which corresponds to the clusters with some atom(s) in Ta_4^+ replaced by Nb and/or W atom(s), was also found to be quite stable, as long as the total number of atoms is 4. The same magic stoichiometries are also observed for $Ta_nNb_mMo_k^+$, as can be seen in Figure 3b.

Similar experiments were performed for the clusters composed of both group A and group B elements. Figure 3c shows the abundance of $Ta_nNb_mAl_k^+$. The cross-sectional plot at $k = 0$ shows a diagonal line at $n + m = 4$ again. However, the diagonal line for $k = 1-3$ does not shift with the number of Al atoms. This finding suggests that $Ta_nNb_m^+$ ($n + m = 4$, with $n \geq 1$) is so stable that the inclusion of the Al atoms into the stable structure is unfavorable. The Al atoms are likely to attach onto the surface of $Ta_nNb_m^+$. The same trend was observed for $Ta_nNb_mPt_k^+$, $Ta_nNb_mCo_k^+$, and $Ta_nW_mAl_k^+$, as shown in Figures 3c−g. Figure 3h shows the abundance of $Ta_nV_mAl_k^+$. In contrast to the other cases, there is no explicit diagonal line. There is a line parallel to the axis at $n = 4$, suggesting that $Ta_4V_mAl_k^+$ are abundantly formed in the gas phase. The experimental results were summarized as follows. Clusters consisting of Ta and other group A elements readily form the stable tetramer. The group B

dx.doi.org/10.1021/jp1095932 |J. Phys. Chem. A 2011, 115, 1516–1520

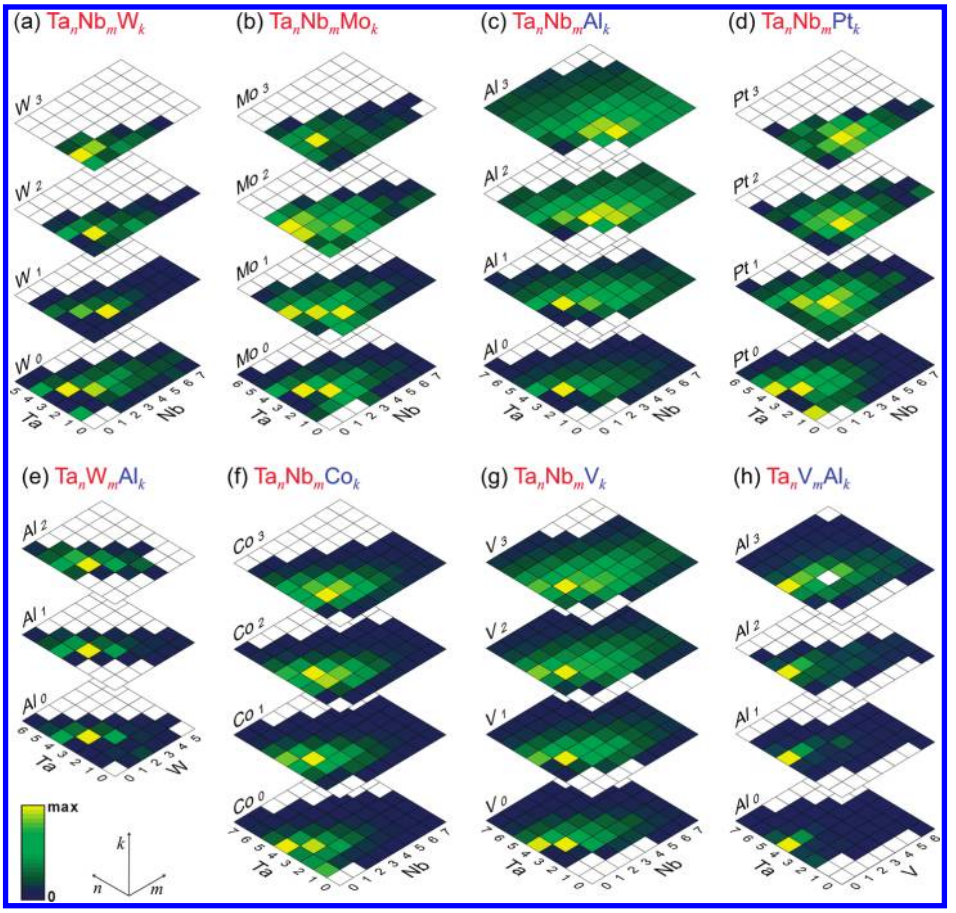

Figure 3. Relative abundances of positive trimetallic cluster ions exhibited in a map as color codes. Each map-element corresponds to a cluster ion, whose stoichiometry is shown by *n*, *m*, and *k*, the number of atoms involved in the cluster. Color scales represent the relative abundance normalized within each layer of *k*: (a) $Ta_nNb_mW_k^+$, (b) $Ta_nNb_mMo_k^+$, (c) $Ta_nNb_mAl_k^+$, (d) $Ta_nNb_mPt_k^+$, (e) $Ta_nW_mAl_k^+$, (f) $Ta_nNb_mCo_k^+$, (g) $Ta_nNb_mV_k^+$, and (h) $Ta_nV_mAl_k^+$.

atoms do not participate in the stable tetramer; instead, they seem to be segregated from the stable structure. We determined that the concept of the two groups of elements can be extended to the trimetallic system.

Thermal Fragmentation of $Ta_nNb_m^+$ Clusters. To confirm the relative stabilities of Ta_4^+ and the substituted ones, a thermal fragmentation experiment, namely, an annealing of clusters, was performed. In the experiment, the temperature of the extension tube at the end part of the cluster source was set to T = 345 and 573 K. Clusters passing through the heated tube absorbed thermal energy via collisions with the buffer He gas atoms, and the thermally unstable clusters with excess energy dissociated to become more-stable clusters by the evaporation of atoms. Mass spectra of $Ta_nNb_m^+$ clusters taken at T = 345 and 573 K, and their difference mass spectrum, are shown in Figure 4a. In Figure 4b, the change in abundance for each cluster by heating was summarized as a color map. As the intensity of the clusters with magic stoichiometry (Ta_4^+, $Ta_3Nb_1^+$, $Ta_2Nb_2^+$, and $Ta_1Nb_3^+$) increased at 573 K, the intensity of the other clusters decreased. Since the ionization energies of the Ta_nNb_m clusters are less than those of the Nb and Ta atoms, evaporation of neutral metal atoms is the dominant process. Via this evaporation process, a cluster loses atoms, until it reaches a stable composition. Hence, we can conclude that the diagonal line in the map along the magic stoichiometry clusters of $Ta_nNb_{4-n}^+$ ($n \geq 1$) indicates their remarkable thermodynamic stability.

$$Ta_nNb_m^+ \xrightarrow{\Delta} Ta_{n'}Nb_{m'}^+ + (n-n')Ta + (m-m')Nb \quad (1)$$

Geometrical Structures Based on Theoretical Studies. The question to be answered is this; Why are the group A atoms permitted to take part in the stable tetramer? Let us discuss the geometrical structures of Ta_4 and the substituted ones. The Lombardi group recorded and analyzed the Raman spectrum of Ta_4 in an argon matrix.[7] They concluded that Ta_4 has a tetrahedral geometry, from the ratio of the observed frequencies. The Metha group optimized the ground-state geometry using the DFT calculation, and showed that Ta_4 has a tetrahedral geometry where the Ta−Ta bond length is 2.548 Å.[8] Fa et al. calculated the ground-state structure of Ta_n clusters and stated that structural transition from 2D to 3D occurred at n = 3−4.[9]

Then, Ta_3Nb, where one Ta atom is replaced by the Nb atom, is almost perfectly pyramidal, with the Ta−Ta bond length being equal to the Ta−Nb bond length (2.543 Å), according to the calculations by the Metha group. In contrast, the geometrical structure of Ta_3V, where one Ta atom is replaced by the V atom, possess C_{3v} symmetry with a Ta−V bond length of 2.413 Å. In addition, Ta_2VNb, which is a tetramer consisting of group A and group B atoms, has open arachno structures, where two Ta atoms

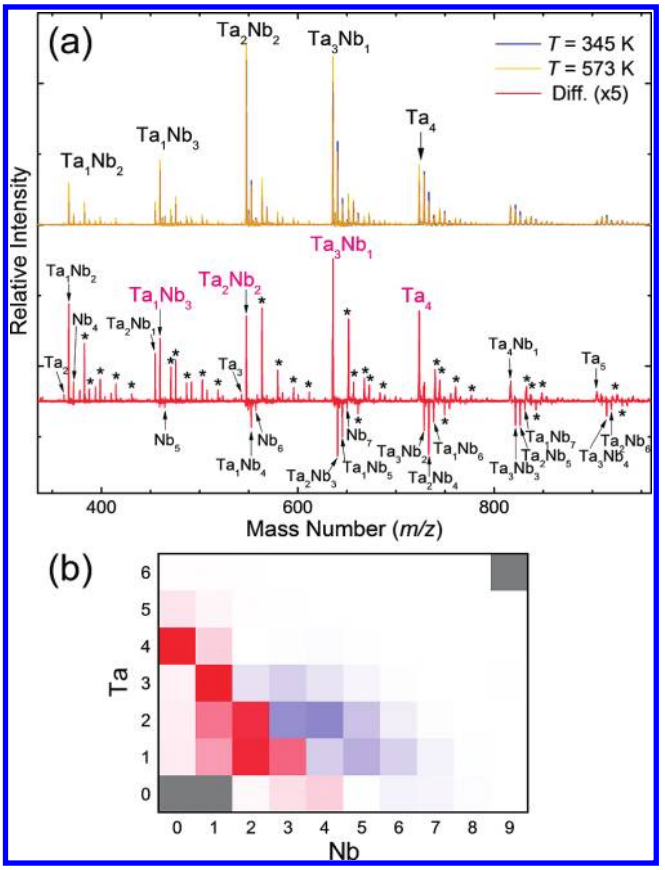

Figure 4. (a) Mass spectra of $Ta_nNb_m^+$ clusters taken at T = 345 and 573 K, and difference mass spectrum obtained at the two temperatures. Peaks labeled with asterisks are assigned as oxidized clusters. (b) Intensity change of $Ta_nNb_m^+$ clusters between two temperatures T = 345 and 573 K exhibited in a map as color codes. Red and blue colors respectively represent the increase and decrease of cluster abundance due to heating.

constitute the wingtips, and the wingtip span is ~3 Å. Considering the geometrical structures of the clusters with the magic stoichiometry, we are able to deduce that the stability of the tetramer is related to the distortion-less tetrahedral structure.

The group A and group B elements are categorized based on the molar heat of vaporization of the bulk materials.[4] Although the dissociation energies or binding energies are dependent on cluster size,[10] there is a rough correlation between the dissociation energies and the molar heat of vaporization (see Figure 5). The binding energy of the atoms of the group B elements is much lower than that of atoms of the group A elements. Our experiments, along with the calculations by the Metha group, suggest that the geometrical structure of a cluster, which is composed of atoms with similar binding energies, is more symmetrical and is free from distortion; hence, they are stable in the gas phase.

From the viewpoint of surface alloy formation, Ruban et al. calculated the segregation energy for various combinations of transition-metal elements.[22] According to the calculated surface segregation energies, many metals should not segregate on the Ta surface. However, no clear difference can be found between the energy values for group A and B elements, as found in this study. It is likely that those values are applicable to the closed-pack surface and not to the small metal cluster. For the case of nanoparticles, Reyes-Nava et al. predicted the stable structures of

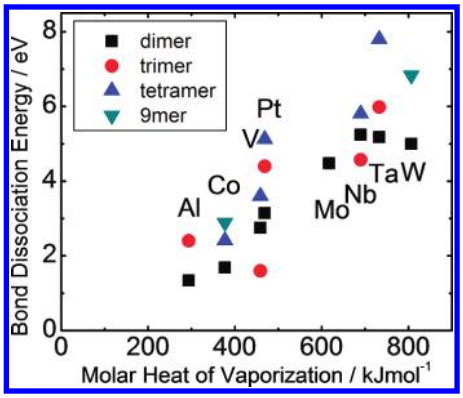

Figure 5. Correlation between the bond dissociation energy and the molar heat of vaporization. Bond dissociation energies[11−20] and molar heat of vaporization values[21] are taken from the literature.

Pt−Au, Pt−Pd, and Pt−Ni bimetallic clusters of 561-atom systems by molecualr dynamics (MD) and DFT calculations.[23] They estimated the cohesive energy of an atom in a cluster from the sum of energies corresponding to the attractive and repulsive interactions with the other atoms of the system. With some assumptions, they presented two useful predictions to determine the stable chemical ordering in a bimetallic cluster. They proposed that, for adjacent elements in a period of the periodic table, the bimetallic system would be more stable if the component with smallest valence electron density is placed onto the surface. They also proposed that, in bimetallic clusters built with elements of only one group, the tendency of the elements with higher core electron density to be located on the surface is higher for those clusters with elements most separated in the group. This prediction may account for the segregation of the Ta−V system seen in this study.

CONCLUSION

Trimetallic cluster ions consisting of Ta and other metal elements were prepared in the gas phase by a triple laser-ablation technique in a controlled manner. We examined the magic stoichiometry of the trimetallic cluster ions and found that clusters consisting of Ta and the other group A elements (Nb, Mo, and W) readily form the stable tetramer. The group B atoms (Al, Co, Pt, and V) do not participate in the stable tetramer; instead, they seem to be separated from the stable structure. Significant stability of magic stoichiometry clusters of $Ta_nNb_m^+$ was found in the thermal fragmentation experiment. It was concluded that the molar heat of vaporization, or the binding energy of clusters, is a useful parameter to categorize the elements for coalescence or segregation in the subnanometer region.

AUTHOR INFORMATION

Corresponding Author

*E-mail: mafune@cluster.c.u-tokyo.ac.jp.

ACKNOWLEDGMENT

This research is supported by Genesis Research Institute, Inc., for the cluster research.

REFERENCES

(1) Hume-Rothery, W.; Mabbott, G. W.; Channel Evans, K. M. *Philos. Trans. R. Soc. London, Ser. A* **1934**, *233*, 1–97.

(2) Gschneidner, K. A., Jr.; Verkade, M. *Prog. Mater. Sci.* **2004**, *49*, 411–428 and references therein.

(3) Alonso, J. A.; Simozar, S. *Phys. Rev. B* **1980**, *22*, 5583–5589.

(4) Miyajima, K.; Fukushima, N.; Himeno, H.; Yamada, A.; Mafuné, F. *J. Phys. Chem. A* **2009**, *113*, 13448–13450.

(5) Sakurai, M.; Watanabe, K.; Sumiyama, K.; Suzuki, K. *J. Chem. Phys.* **1999**, *111*, 235–238.

(6) Nakajima, A.; Hoshino, K.; Naganuma, T.; Sone, Y.; Kaya, K. *J. Chem. Phys.* **1991**, *95*, 7061–7066.

(7) Fang, L.; Shen, X.; Chen, X.; Lombardi, J. R. *Chem. Phys. Lett.* **2000**, *332*, 299–302.

(8) Addicoat, M. A.; Buntine, M. A.; Metha, G. F. *Aust. J. Chem.* **2004**, *57*, 1197–1203.

(9) Fa, W.; Luo, C.; Dong, J. *J. Chem. Phys.* **2006**, *125*, 114305.

(10) Starace, A. K.; Neal, C. M.; Cao, B.; Jarrold, M. F.; Aquado, A.; López, J. M. *J. Chem. Phys.* **2008**, *129*, 144702.

(11) Fu, Z.; Lemire, G. W.; Bishea, G. A.; Morse, M. D. *J. Chem. Phys.* **1990**, *93*, 8420–8441.

(12) Fu, Z.; Lemire, G. W.; Hamrick, Y. M.; Taylor, S.; Shui, J.-C.; Morse, M. D. *J. Chem. Phys.* **1988**, *88*, 3524–3531.

(13) Weidele, H.; Kreisle, D.; Recknagel, E.; Becker, St.; Kluge, H.-J.; Lindinger, M.; Schweikhard, L.; Walther, C.; Ziegler, J. *J. Chem. Phys.* **1999**, *110*, 8754–8766.

(14) Miller, S. R.; Schultz, N. E.; Truhlar, D. G.; Leopold, D. G. *J. Chem. Phys.* **2009**, *130*, 024304.

(15) Hales, D. A.; Su, C.-X.; Lian, L.; Armentrout, P. B. *J. Chem. Phys.* **1994**, *100*, 1049–1057.

(16) Gutsev, G. L.; Bauschlicher, C. W., Jr. *J. Phys. Chem. A* **2003**, *107*, 4755–4767.

(17) Simard, B.; Lebeault-Dorget, M.-A.; Marijnissen, A.; ter Meulen, J. J. *J. Chem. Phys.* **1998**, *108*, 9668–9674.

(18) Collings, B. A.; Rayner, D. M.; Hackett, P. A. *Int. J. Mass Spectrom. Ion Processes* **1993**, *125*, 207–214.

(19) Grushow, A.; Ervin, K. M. *J. Chem. Phys.* **1997**, *106*, 9580–9593.

(20) Miller, S. R.; Schultz, N. E.; Truhlar, D. G.; Leopold, D. G. *J. Chem. Phys.* **2009**, *130*, 024304.

(21) Dean, J. A. *Lange's Handbook of Chemistry*, 15th ed.; McGraw–Hill: New York, 1999.

(22) Ruban, A. V.; Skriver, H. L.; Nørskov, J. K. *Phys. Rev. B* **1999**, *59*, 15990–16000.

(23) Reyes-Nava, J. A.; Rodríguez-López, J. L.; Pal, U. *Phys. Rev. B* **2009**, *80*, 161412.